Journal of Geospatial Science and Analytics

Journal homepage:
https://ejournal.foundae.com/index.php/jgsa/index
e-ISSN: 3090-8086 | p-ISSN: 3090-532X

Spatio-temporal modeling of built-up land expansion (2005–2055) in the eruption prone area of Gamalama volcano, Ternate island, Indonesia

Heinrich Rakuasa*
National Research Tomsk State University, Russian Federation

Vadim V Khromykh
National Research Tomsk State University, Russian Federation

Article Info

Article history:

Received: July 29, 2025
Revised: Sept 08, 2025
Accepted: Oct 28, 2025

Keywords:

Built-Up Land,
CA MC
Gamalama
Ternate

DOI:
10.58524/jgsa.v1i3.40

Abstract

Ternate Island, a volcanic island dominated by the still-active Gamalama Volcano in North Maluku Province, Indonesia, faces complex dynamics in built-up area development driven by accelerated demographic growth and economic activities, particularly in the trade and tourism sectors. The limited availability of flat land has resulted in increasingly intensive expansion of settlements and infrastructure on the volcanic slopes, areas inherently characterized by high volcanic hazard vulnerability. This study employs a Cellular Automata-Markov Chain modeling approach based on multi-temporal satellite imagery and driving variables, including elevation, slope, distance to road networks, and economic center locations, to analyze land cover change dynamics during the periods 2005, 2015, and 2025 and to model projections for 2035, 2045, and 2055. The results demonstrate significant expansion of built-up land from 2005 to 2055. The rate and spatial distribution of built-up land development within disaster-prone zones Prone Zones I and II underscore the urgency of implementing risk-based spatial planning policies, including stringent restrictions on development in hazardous areas, the development of adequate evacuation infrastructure, and the enhancement of community preparedness capacity. The contributions of this research are highly relevant to sustainable regional planning in tropical volcanic areas with high disaster risk, while also emphasizing the importance of integrating disaster mitigation strategies and climate change adaptation into the spatial planning policies of Ternate Island.

To cite this article: Rakuasa, H., & Khromykh, V. V. (2025). Spatio-temporal modeling of built-up land expansion (2005–2055) in the eruption-prone area of Gamalama Volcano, Ternate Island, Indonesia. *Journal of Geospatial Science and Analytics*, 1(3), 167–184.

***Corresponding Author:**
Heinrich Rakuasa, National Research Tomsk State University, Russian Federation, RUSIA,
Email: heinrich.rakuasa@yandex.ru

INTRODUCTION

Ternate Island, a small volcanic island in North Maluku Province with an area of approximately 101 km² and dominated by the presence of the still-active Gamalama Volcano, is facing significant pressure on built-up land development due to the high rate of economic growth driven by the trade and tourism sectors (Umanailo et al., 2017). The limited land carrying capacity of the island has caused a sharp increase in demand for space for settlements, economic activities, and infrastructure (Sihasale et al., 2023). Data from the Central Statistics Agency shows that Ternate City experienced a population growth rate exceeding 2.5% per year from 2010 to 2023, making it one of the most densely populated cities in Eastern Indonesia, with a density of around 4,600 people per km² (BPS, 2024). This condition has resulted in the shrinking of green open spaces and disaster buffer zones in coastal areas as well as around the slopes of Gamalama Mountain, thereby spatially escalating built-up land, implying increased exposure of the community to geological hazard risks such as volcanic eruptions, lahar flows, and tsunami threats (Hidayat et al., 2022).

Gamalama Mountain, with an elevation of 1,715 meters above sea level, has experienced more than 70 eruptions since the 16th century, with the most recent eruptions occurring in 2011, 2014, and 2018 (BMKG, 2019). The two most densely populated districts on Ternate Island, namely Ternate Tengah and Ternate Utara, are located on the southern slopes of the mountain and are classified as high-hazard disaster-prone zones. Based on a multi-hazard simulation model developed by Hidayat et al., (2022), approximately 34% of the residential areas in these two districts are potentially affected by pyroclastic flows and rain-triggered lahars in the event of an eruption with a Volcanic Explosivity Index (VEI) ≥ 3. Nevertheless, the pressure for built-up land development continues to increase toward the slopes of Gamalama, largely driven by the limited availability of alternative flat land elsewhere on the island, thus posing significant challenges for disaster risk management and sustainable spatial planning (Ham, 2024; Rakuasa, 2025).

Land cover changes on Ternate Island have exhibited highly significant spatio-temporal dynamics over the past two decades. An analysis conducted by Rakuasa & Pakniany (2022), employing the Cellular Automata-Markov (CA-Markov) method, revealed that the built-up land area in Ternate Tengah District increased by 2.3 times between 2002 and 2022, with a projection reaching approximately 1,130 hectares by 2032. Conversion of open land and vegetated areas into residential zones has occurred at an average annual growth rate of 4.2%, which is the highest increase compared to other districts in Ternate City. This finding is corroborated by research by Latue & Rakuasa, (2024), using Sentinel-2 satellite imagery, which identified a radial expansion pattern of built-up areas from the city center toward the slopes at the foot of Gamalama Mountain, resulting in the narrowing of natural buffer zones that function as mitigation buffers against volcanic hazard risks (Kusrini et al., 2023). This condition underscores the necessity for more effective spatial planning interventions to maintain ecological functions and reduce the vulnerability of these areas to disaster threats (Handayani et al., 2022).

A significant imbalance between land availability and spatial demand on Ternate Island has fostered urban sprawl, both vertically through multi-story development on the slopes and horizontally through coastal reclamation (Rakuasa & Khromykh, 2025). Marasabessy, (2016), notes that the waterfront city project in Teluk Toboko successfully added approximately 18 hectares of new land from 2015 to 2020; however, this reclamation activity simultaneously accelerated sedimentation processes and diminished the natural coastal functions in attenuating tsunami waves. Furthermore, a study by Ervita et al., (2019), estimates that sea-level rise of 0.4–0.6 meters by 2050, combined with ongoing intensive reclamation, could submerge around 8% of residential areas in the western coastal region of Ternate Island, posing serious threats to safety and residential continuity in the area. This situation affirms the necessity of an integrated spatial governance approach that incorporates climate change mitigation and coastal disaster risk management comprehensively.

Within the framework of risk-sensitive spatial planning, controlling the spatial dynamics of built-up land development is crucial to reducing regional vulnerability to various natural hazards. A multi-hazard risk assessment approach highlighted by Ma'muri et al., (2025), emphasizes the importance of simultaneously integrating spatial data on volcanic hazards, cold lahar flows, tectonic earthquakes, and tsunamis in spatial planning processes to enhance regional resilience. Despite revisions in the Regional Spatial Plan 2012–2032 concerning the boundaries of disaster-prone zones on Ternate Island, policy implementation faces major challenges due to strong pressures from property and tourism sectors that drive land exploitation in high-risk areas. As a solution, Ubink & Pickering, (2024), propose the development of spatial models based on carrying capacity that consider maximum population density limits and safe distance buffers from the summit of Gamalama Mountain, as a strategic effort to ensure more sustainable and disaster-resilient development in the region.

This study employs the Cellular Automata-Markov Chain (CA-MC) method to analyze the dynamics of land cover changes on Ternate Island for the years 2005, 2015, and 2025, utilizing hazard zone maps of the Gamalama volcanic eruption as primary parameters. Additionally, the study predicts built-up land development for the periods 2035, 2045, and 2055, particularly within disaster-prone areas, enabling risk mapping and evidence-based spatial planning recommendations. Given the complex interactions among rapid development dynamics, the limited physical capacity of a small island, and the potential for recurrent multi-hazard events on Ternate Island, further research is necessary to quantify spatio-temporal critical points where significant built-up land expansion may reduce the resilience of the local social-ecological system. Through spatio-temporal modeling of built-up land changes in 2005, 2015, 2025, 2035, 2045, and 2055, this study aims to make a significant contribution to the development of regional planning science and disaster risk adaptation in tropical volcanic island settings.

METHOD

1. Research Locations and Data Collection

This study was conducted on Ternate Island, encompassing the eruption-prone area of Mount Gamalama, North Maluku Province, Indonesia. Geographically, Ternate Island is situated between 0° and 2° North Latitude and 126° to 128° East Longitude and is bordered as follows: to the north by the Maluku Sea, to the south by the Maluku Sea, to the east by the Halmahera Strait, and to the west by the Maluku Sea. The research location is illustrated in Figure 1.

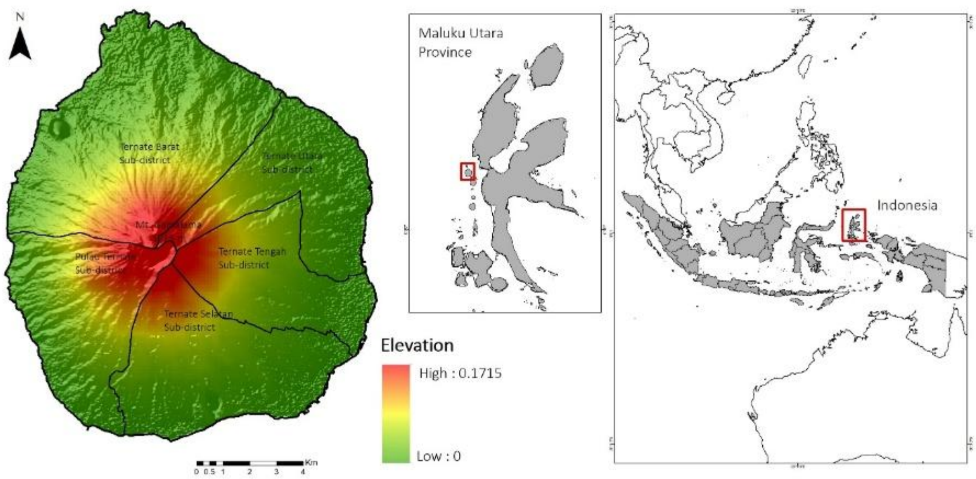

Figure 1. Research Location: Ternate Island, Indonesia

The research data used in this study consist of data for land cover change analysis, driving variables to predict built-up land development, and hazard-prone areas of Gamalama Volcano eruptions. The data utilized for land cover change analysis were Landsat 5 and Landsat 8 OLI/TIRS satellite imagery obtained from the United States Geological Survey for the periods 2005, 2015, and 2025. Data for driving variables related to built-up land development included road network data and distance from economic centers obtained from the Indonesian topographic maps, as well as elevation and slope data derived from the National DEM sourced from the Geospatial Information Agency. Data on the hazard-prone areas of Gamalama Volcano eruptions were obtained from the National Disaster Management Agency. Data processing in this study was conducted using several software packages, including ENVI, ArcGIS Pro, Google Earth, IDRISI Selva, and Microsoft Excel. The data processing involved the creation of land cover maps for the years 2005, 2015, and 2025; the development of driving variables consisting of elevation, slope, distance from roads, and distance from economic activity centers; and the production of predictive land cover maps for 2035, 2045, and 2055, which were then overlaid with the hazard-prone area maps of Gamalama Volcano eruptions to analyze built-up land development within these areas.

2. Land Cover Data Processing

Land cover data processing began with processing Landsat-5 TM and Landsat 8 OLI/TIRS imagery, specifically through radiometric calibration. Radiometric calibration was conducted in two stages: The first involved converting Digital Number (DN) values to radiance using Equation (1):

$$L\lambda = \frac{LMAX\lambda - LMIN\lambda}{QCalMAX - QCalMIN} * (QCal - QCalMIN) + LMIN\lambda. \quad (1)$$

With: Lλ = spectral radiance at the sensor ($W/m^2 \cdot sr \cdot \mu m$), LMAXλ = spectral radiance scaled to QCalMAX ($W/m^2 \cdot sr \cdot \mu m$), LMINλ = spectral radiance scaled to QCalMIN ($W/m^2 \cdot sr \cdot \mu m$), QCalMAX = maximum calibrated quantized pixel value (DN = 255), QCalMIN = minimum calibrated quantized pixel value (DN = 1), QCal = calibrated pixel value (DN). After converting DN to radiance, the second step is to convert the radiance value to reflectance using Equation (2).

$$\rho\lambda = \frac{\pi * L\lambda * D^2}{ESUN\lambda * \mathrm{Cos}\theta}. \quad (2)$$

With: ρλ = the reflectance value of the object at the sensor, π = the constant pi (3.14), Lλ = spectral radiance at the sensor ($W/m^2 \cdot sr \cdot \mu m$), D = Earth-Sun distance (astronomical units), ESUNλ = mean solar exoatmospheric spectral irradiance, θ = solar zenith angle (90° minus the solar elevation angle). Radiometric calibration for Landsat 8 OLI/TIRS only involves converting the Digital Number (DN) values directly into reflectance values using Equation (3).

$$\rho\lambda = (\mathrm{M\rho} * \mathrm{Qcal}) + A\rho. \quad (3)$$

With: ρλ = the reflectance value of the object at the sensor, Mρ = scale factor, Aρ = additive factor, and Qcal = pixel value (N).

The satellite imagery that has undergone radiometric calibration is then processed using natural color band composites to facilitate the interpretation and digitization process in ArcGIS Pro software. Prior to interpretation, the three images are clipped according to the study area boundary. Interpretation is conducted based on the visual appearance of the satellite images, concurrently validated with PlanetScope imagery. The land cover classification follows SNI

7465:2010, which consists of built-up land, open land, agricultural land, and water bodies (Badan Standarisasi Nasional, 2010).

3. Driving Factor Data Processing

The driving variables for built-up land development used in this study are elevation, slope, distance from roads, and distance from economic centers (Figure 2). Each driving factor is classified and assigned weights according to the probability of land cover change occurrence. In this context, scoring is applied to each driving factor to determine the suitability level for settlement development in the area (Supriatna et al., 2022). Areas with higher suitability receive higher scores, while less suitable areas receive lower scores. The lower the score, the lower the likelihood of settlement development; conversely, the higher the score, the higher the likelihood of built-up land expansion in the respective areas (Somae et al., 2023; Achmadi et al., 2023). These four driving factors were processed using ArcGIS Pro software with the Classify, Slope, and Multi Ring Buffer tools, followed by fuzzy overlay techniques. The fuzzy logic technique formalizes approximate reasoning by representing it in a continuous range from 0 to 1, which is an effective approach for cellular automata-based modeling (Espitia et al., 2021).

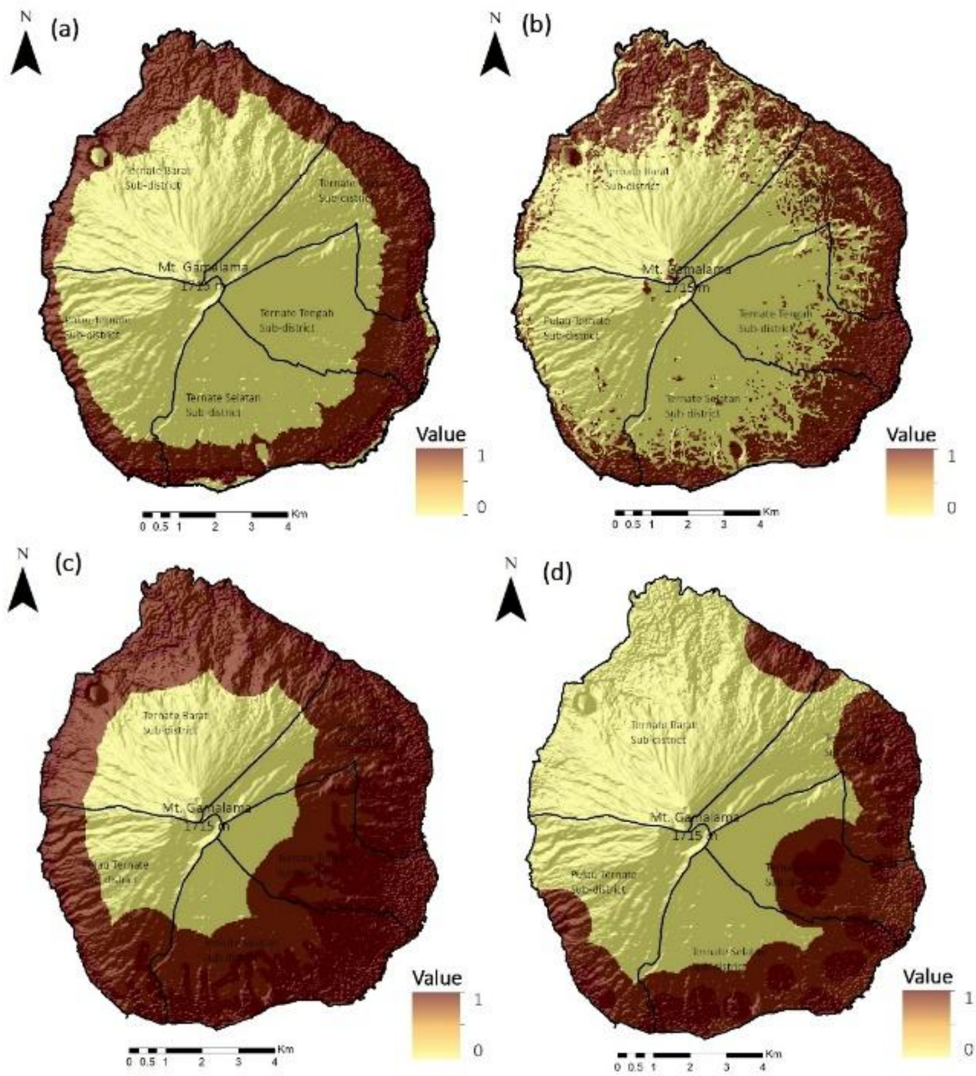

Figure 2. Driving Variables: (a) Elevation, (b) Slope, (c) Distance from Roads, (d) Distance from Economic Centers.

4. Future Land Cover Prediction

This study employs the Cellular Automata-Markov Chain (CA-MC) approach. The Cellular Automata-Markov Chain (CA-MC) is a hybrid model commonly used to investigate changes in land use and/or land cover (Al-Shaar et al., 2021). This model combines the advantages of the long-term predictive capability of the Markov model with the ability of Cellular Automata (CA) to effectively simulate changes in land use and/or land cover (Latue & Rakuasa, 2023; Abdelsamie et al., 2024; Mirzakhani et al., 2025). The characteristics of the Markov Chain process are suitable for application to dynamic land changes and exhibit various properties of Markov processes. The transition probability matrix of land cover is defined by Equation (4).

$$P = (Pij), \tag{4}$$

where: Pij represents the probability of land cover change and n denotes the number of land use types. Pij must satisfy the conditions outlined in Equations 5 and 6.

$$0 \leq P \leq 1 (i, j = 1,2,3, \ldots, n) \tag{5}$$

$$\sum_{j=1}^{n} Pij = 1, (i, j = 1,2,3, \ldots, n) \tag{6}$$

Based on the transition probability matrix and Bayes' theorem, the Markov Chain prediction model is as follows:

$$P(n) = P(n-1)Pij, \tag{7}$$

where: P(n) represents the transition probability at a given time, and P(n-1) represents the probability at the previous time (initial).

Markov Chain alone is insufficient for predicting and simulating land cover dynamics because it does not consider the spatial distribution of each land category or the direction of spatial growth (Fachruddin et al., 2025). The Cellular Automata model is combined with the Markov Chain to incorporate spatial structure and geographical direction in land use change (Mirzakhani et al., 2025). Cellular automata function to add spatial characteristics to the model (Xing et al., 2020). Cellular automata constitute a discrete dynamic system where the state of each cell at time t+1 is determined by the states of its neighboring cells at time t according to predetermined transition rules (Fitri et al., 2021). Cellular automata possess dynamic and spatial properties, making them an ideal choice for representing spatial and dynamic processes. GIS and cellular automata models are integrated for dynamic land change simulation and can generate simulated land cover patterns with realistic spatial structures (Kura & Beyene, 2020). The cellular automata model interacts over time and consists of four main components, namely:

$$U, S, N, T, \tag{8}$$

where: U = universe or cell space, S = states or possible states that a cell can achieve, N = neighborhood or the number of neighboring cells influencing the state of a cell, T = transition or the rules used to determine the state of a cell.

Land cover modeling for the years 2025, 2035, 2045, and 2055 was conducted using the IDRISI Selva software, beginning with the analysis of previous land cover transitions using the Land Change Modeler tool. Subsequently, a transition probability matrix was generated with the Markov Chain tool by simulating land cover changes in 2025 based on the period 2005–2015. Following this, the 2025 land cover simulation was produced from the 2005–2015 data using the Cellular Automata-Markov Chain tool. The modeled land cover for 2025 was then validated against the existing 2025 land cover using the Validate tool within IDRISI Selva software. This validation aimed to determine the accuracy level of the model. Validation testing was based on the Kappa statistic (Equation 9), where a Kappa value above 0.75 (75%) indicates that the simulation model is valid and can be used for modeling land cover for 2035, 2045, and 2055 (Ghalehteimouri et al., 2022). The final process involved developing predictive land cover models for 2035, 2045, and 2055 using the available driving variables.

$$Kappa\ Accuracy = \frac{N\ \sum_{i=1}^{r} xii - \sum_{i=1}^{r}(x_{1+} + Xx + i)}{N^2\ \sum_{i=1}^{r}(x_{i+} + Xx + i)}, \tag{9}$$

where: Xi = area of land use type i from observation, xi+ = area of land use type i from simulation, xii = area of land use type i from simulation corresponding to the observed area of land use type i, I = rows and columns, r = number of land use types, N = total area of all land use types.

5. Data Processing of the Eruption-Prone Area of Gamalama Volcano

The data processing for Gamalama Volcano's eruption-prone area utilizes the JPG-format Eruption Hazard Zone Map of Gamalama Volcano obtained from the Directorate of Volcanology. The processing was conducted using ArcGIS 10.8 software, beginning with geometric correction to align the coordinate system with other spatial data. This was followed by digitization to obtain vector-format eruption hazard zone data (Shapefile). This step is essential to facilitate the overlay process between built-up land data and Gamalama Volcano's eruption hazard zone data.

6. Built-Up Land Expansion Prediction in the Eruption-Prone Area of Gamalama Volcano

The prediction of built-up land expansion in the eruption hazard zone of Mount Gamalama is carried out by combining built-up land data from various years (2005, 2015, 2025, 2035, 2045, and 2055) with the eruption hazard zone data of Mount Gamalama using the intersect function in ArcGIS 10.8 software. This intersect method enables spatial overlay analysis to determine the extent to which the built-up land area has expanded within or overlaps with the eruption hazard zone of the volcano.

The process begins with collecting built-up land maps for the specified years, then projecting these data into a geographic information system for overlaying with the eruption hazard zone map of Mount Gamalama. The intersection results from these two datasets will provide information about the changes and expansion of development areas that may be impacted by eruption hazards. This analysis is crucial for disaster risk mitigation planning and spatial management to ensure that development does not increase the risk of natural hazards in these eruption-prone areas.

RESULTS AND DISCUSSIONS

1. Land Cover of Ternate Island in 2005, 2015, 2025

Land cover analysis of Ternate Island shows significant changes over the past two decades. In 2005, the majority of the land was dominated by agricultural areas (80.35%) with built-up areas covering 1,543.61 hectares (15.19%). However, by 2015, built-up areas increased to 1,857.69 hectares (18.28%) while agricultural land decreased to 7,904.98 hectares (77.79%). This trend continued in the 2025 projection, where built-up land is estimated to rise to 2,120.46 hectares (20.87%) and agricultural land to decline to 7,596.93 hectares (74.75%), as detailed in Table 1. These dynamics reflect patterns of urbanization and expansion of urban areas that are common characteristics in many island regions and cities in Southeast Asia, driven by population growth and increasing infrastructure needs (Mao et al., 2023; Kamarajugedda et al., 2023).

Table 1. Area of Land Cover on Ternate Island in 2005, 2015, 2025

LULC	Area 2005		Area 2015		Area 2025	
	Ha	%	Ha	%	Ha	%
Build-up Land	1.543,61	15,19	1.857,69	18,28	2.120,46	20,87
Opened Land	385,36	3,79	331,87	3,27	377,67	3,72
Agricultural Land	8.165,80	80,35	7.904,98	77,79	7.596,93	74,75
Water Body	67,58	0,67	67,58	0,67	67,58	0,66
Total Area	10.162,35	100,00	10.162,35	100,00	10.162,35	100,00

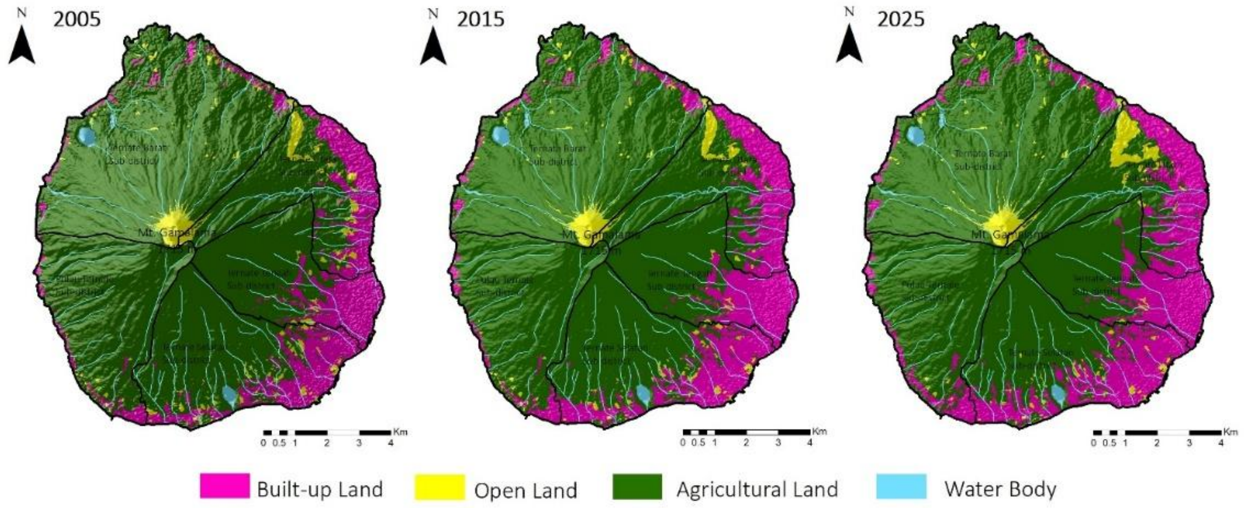

Figure 3. Land Cover of Ternate Island in 2005, 2015, 2025

The conversion of agricultural land into built-up areas has significant implications for food security and the local economy. Studies in Palembang and the northern coast of West Java show that agricultural land conversion leads to a decline in farmers' welfare, disrupts regional food security, and increases dependency on food supplies from outside sources (Yuliantina et al., 2024; Gandharum et al., 2024). Furthermore, uncontrolled conversion can heighten vulnerability to disasters, especially in areas prone to volcanic eruptions, such as the slopes of Mount Gamalama. This phenomenon underscores the urgency of implementing sustainable agricultural land protection policies and spatial planning based on disaster mitigation to minimize ecological and socio-economic losses (Bachri et al., 2024).

The predicted increase in built-up areas in volcanic eruption-prone disaster zones also has the potential to increase the exposure of populations and infrastructure to disaster risks. Simulation studies in volcanic eruption-affected areas in New Zealand and Indonesia emphasize the need for adaptive spatial planning, including mitigation zoning, to ensure that urbanization does not exacerbate disaster impacts in the future (Cardwell et al., 2021). Therefore, spatial utilization management in disaster-prone areas must adopt a spatial-temporal data-based and future prediction approach, as done in this study, to support sustainable development policies and minimize disaster risks for the communities of Ternate Island.

2. Validation of the 2025 land cover model with the existing 2025 land cover

In this study, the accuracy of the 2025 land cover prediction was tested against the existing (actual) 2025 land cover using Kappa index validation. Validation with the Kappa index can show and determine the degree of agreement between the land cover model (the predicted land cover for 2025) and the existing land cover (land cover derived from digitization verified with high-resolution imagery). This process is conducted to understand the accuracy level of the developed model. The maximum Kappa value, considering the number of rows and columns, is 1.00. In Figure 4, which presents the validation of the prediction model using the Kappa test, there is a Kstandard value that indicates the accuracy level of the developed model. In this study, the

Kstandard value was 0.7643 or 76%, meaning the accuracy level is considered very good since the result is greater than 75% (Wang et al., 2022). This very good accuracy result confirms the model design to be continued into land cover models for 2035, 2045, and 2055. The Kappa test results can be seen in Table 2.

Table 2. Kappa Test Results of the 2025 Model in IDRISI Selva Software

Variables	Value
Kstandard	***= 0.7643 or 0,76%***
Kno	= 0.8588
Klocation	= 0.8182
KlocationStrata	= 0.8182

3. Land cover prediction results for 2035, 2045, and 2055 using the Cellular Automata-Markov Chain

The land cover prediction results for 2035, 2045, and 2055 using the Cellular Automata-Markov Chain (CA-Markov) method in the volcanic eruption-prone area of Mount Gamalama, Ternate Island, show a significant trend in land composition changes up to 2055. The 2035 projection indicates the built-up land area reaching 2,553.68 hectares (25.13%), open land at 329.92 hectares (3.25%), agricultural land at 7,210.82 hectares (70.96%), and water bodies covering 67.58 hectares (0.67%). These figures show that the expansion of built-up land continues to increase in line with the growing space demands driven by population growth and economic activities, which encourage the conversion of agricultural and open land into settlements (Gharaibeh et al., 2020; Yaagoubi et al., 2024). The land cover prediction results for 2035, 2045, and 2055 can be seen in Figure 4.

In 2045 and 2055, the CA-Markov projection shows a consistent accumulation of land changes, with built-up land growing to 2,768.50 hectares (27.25%) in 2045 and further increasing to 3,090.05 hectares (30.41%) in 2055. Meanwhile, agricultural land decreases from 7,210.82 hectares (2035) to 6,677.53 hectares (2055), reflecting a significant land conversion process. The conversion of agricultural land into built-up areas is a common phenomenon in developing regions and has been identified in various contexts across Indonesia, especially in coastal areas near economic centers and on volcanic islands like Ternate (Kusrini et al., 2023; Yaagoubi et al., 2024). This reduction in agricultural land not only impacts food security but also increases community exposure to natural disaster risks, considering that much of the built-up land may lie within zones prone to eruptions and landslides. The complete land cover area of Ternate Island for the years 2035, 2045, and 2055 can be seen in Table 3.

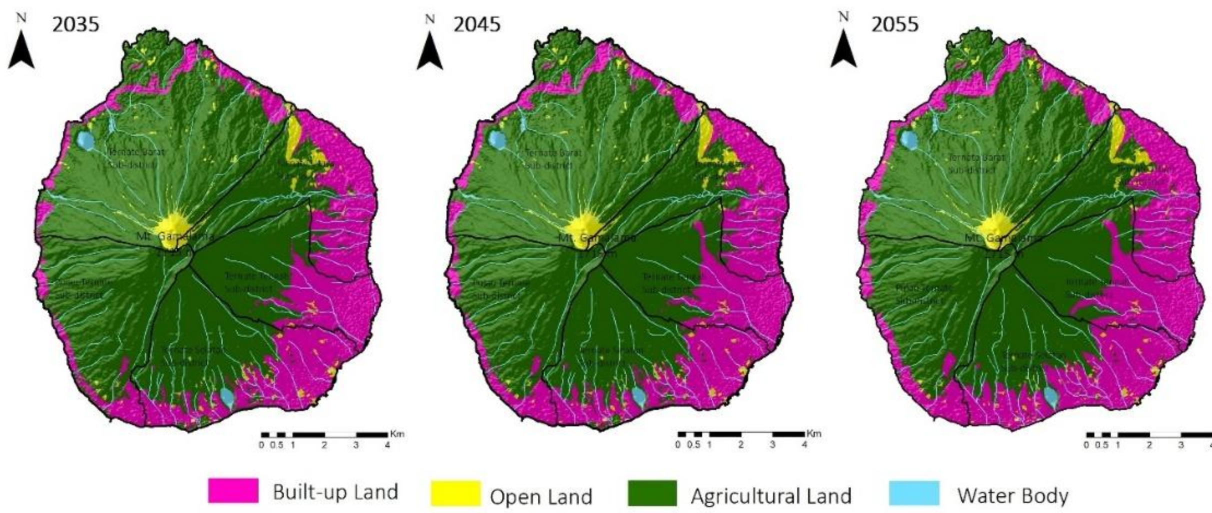

Figure 4. Land Cover Prediction Results for the Years 2035, 2045, and 2055

Table 3. Land Cover Area of Ternate Island in 2035, 2045, and 2055

LULC	Area 2035		Area 2045		Area 2055	
	Ha	%	Ha	%	Ha	%
Build-up Land	2.553,68	25,13	2.768,50	27,25	3.090,05	30,41
Open Land	329,92	3,25	331,22	3,26	327,57	3,22
Agricultural Land	7.210,82	70,96	6.992,56	68,83	6.677,53	65,71
Water Body	67,58	0.67	67,58	0,67	67,58	0,66
Total Area	10.162,35	100,00	10.162,35	100,00	10.162,35	100,00

The trend of built-up land expansion in Ternate aligns with previous studies that highlight the accuracy and effectiveness of the CA-Markov approach in simulating spatial and temporal land use changes (Yaagoubi et al., 2024). This model can capture land transition dynamics and realistically estimate pressures from population growth and economic dynamics (Salakory & Rakuasa, 2022). In the context of the disaster-prone Gamalama area, these prediction results are crucial to be considered in preparing adaptive spatial planning policies, disaster risk mitigation, and the preservation of agricultural land functions in the future. Policies for controlling development in high-risk zones and optimizing the use of marginal land need serious attention to ensure sustainable development on Ternate Island is maintained.

4. Development of Built-up Land on Ternate Island from 2005 to 2055

The development of built-up land in the volcanic eruption hazard zone of Mount Gamalama shows a consistent and significant growth trend from 2005 to the projected year 2055. The built-up land area increased from 1,543.61 hectares in 2005 to 1,857.69 hectares in 2015 and is projected to continue rising to 2,120.46 hectares in 2025. This sharp increase continues to 2,553.68 hectares in 2035 and 2,768.50 hectares in 2045 and is estimated to reach 3,090.05 hectares by 2055. These data reflect a high rate of urbanization, in line with urban growth patterns characteristic of various regions in Indonesia, especially areas experiencing demographic pressures and large land demands due to population growth and local economic dynamics (Rakuasa, 2025). The graph of built-up land development for the years 2005, 2015, 2025, 2035, 2045, and 2055 can be seen in Figure 5.

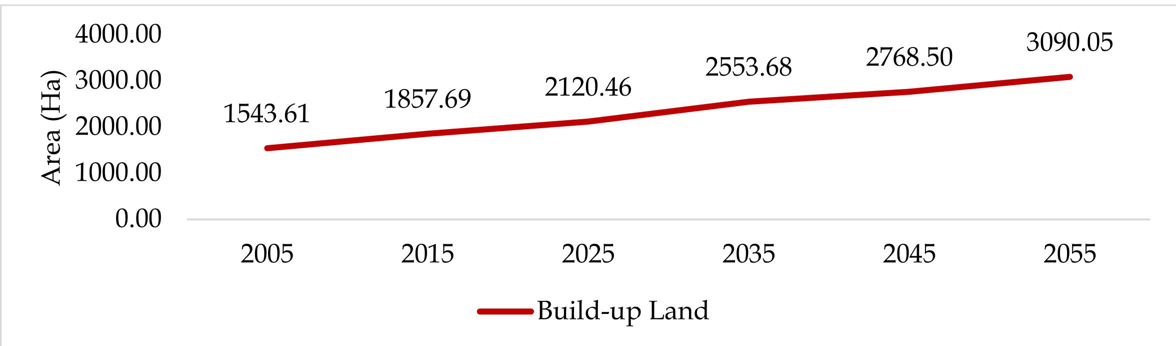

Figure 5. Graph of Built-up Land Development for the Years 2005, 2015, 2025, 2035, 2045, and 2055

The growth pattern of built-up land shows that the pressure for land conversion especially from agricultural or open land to built-up land will increase significantly in the coming decades. This phenomenon is driven by the expansion of settlements, infrastructure development, and the demand for urban space in island areas with potential volcanic disaster risks. Prediction models using spatial-temporal approaches such as the Cellular Automata-Markov Chain have proven effective in capturing the dynamics and trends of land use transition accurately, with model validation in various studies showing over 90% accuracy in projecting LULC changes several decades ahead. These findings underscore the importance of risk-based spatial planning management and the integration of mitigation policies to anticipate the increasing exposure of built-up land in the volcanic hazard zones of Mount Gamalama in the future.

5. Disaster-Prone Area of Mount Gamalama Volcanic Eruption

The Eruption Hazard Map of Mount Gamalama on Ternate Island, shown in Figure 6 and obtained from the Directorate of Volcanology, Ministry of Energy and Mineral Resources, divides the area into three zones based on the level of threat and its extent: Hazard Zone I covering an area of 1,072.19 hectares, Hazard Zone II covering 1,719.40 hectares, and Hazard Zone III covering 1,012.51 hectares. This zoning is based on geomorphological analysis, eruption history, and the potential flow of eruption products such as lava, pyroclastic flows, and volcanic materials. Areas classified as Hazard Zones I and II generally face direct exposure to primary impacts like lava flows and pyroclastic density currents, whereas Hazard Zone III tends to be affected by secondary threats such as ashfall or lahars.

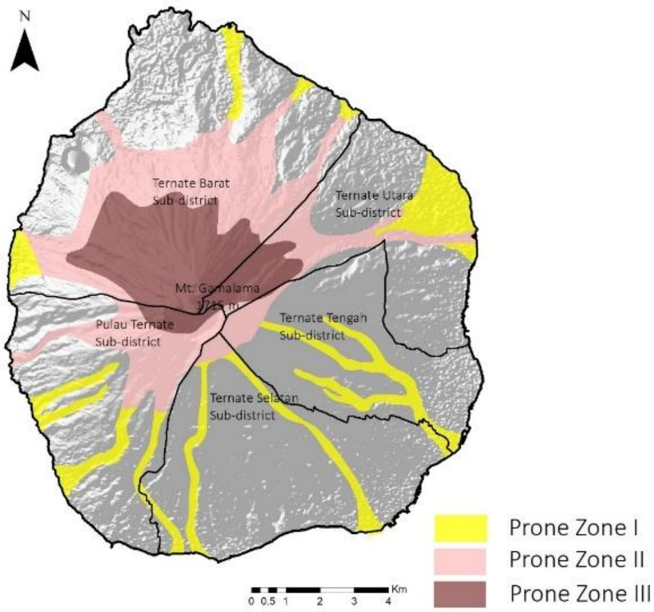

Figure 6. Disaster-Prone Area of Mount Gamalama Volcanic Eruption

In the context of Ternate, the physical and social vulnerability of communities in these hazard zones is very high, given the settlement patterns where many residents concentrate on the hills surrounding Mount Gamalama's body and the relatively short distance between the mountain base and residential areas. Research shows that approximately 42.38% of villages on Ternate Island fall into the high vulnerability category due to their proximity to the volcano and limited effective evacuation routes (Tyas Wulan Mei et al., 2017). Moreover, infrastructure such as roads, evacuation facilities, and public amenities are often located within these hazard zones, increasing the potential socio-economic impact if a major eruption occurs. This situation highlights the necessity for integrating spatial data, hazard zoning maps, and disaster mitigation-based spatial planning into all regional development policies.

The hazards of the Gamalama eruption are not limited to pyroclastic material ejections and lava flows but also include secondary threats such as ashfall and lahars that can suddenly affect Zones I through III. For example, the eruption history in 2011 and 2014 produced eruptions with volcanic material reaching beyond the core zones, causing significant disruption to public infrastructure and the socio-economic activities of the Ternate community (Lessy et al., 2024). Therefore, area protection, evacuation planning, and community preparedness must be top priorities, especially for the more than 3,800 hectares covering all three hazard zones.

6. Prediction of Built-up Land Development in the Volcanic Eruption Hazard Zone of Mount Gamalama

Spatial-temporal analysis of the predicted built-up land development in the volcanic eruption hazard zone of Mount Gamalama shows a consistent growth trend from 2005 to the projected year 2055. Prone Zone I recorded a significant increase from 343.11 hectares in 2005 to 581.43 hectares in 2055. A similar trend occurred in Prone Zone II, rising from 29.42 hectares to 65.97 hectares during the same period. This phenomenon reflects the increasing urbanization pressure in peripheral areas classified as disaster-prone, in line with the global trend where urban growth, especially in developing countries, drives the expansion of built-up land into high-risk hazard zones (Lessy et al., 2024).

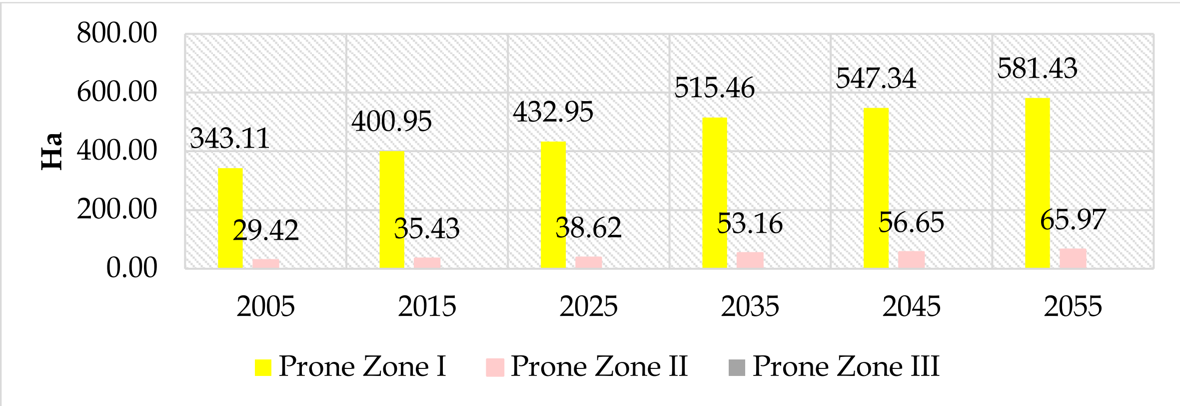

Figure 7. Built-up Land Area in the Volcanic Eruption Hazard Zone of Mount Gamalama

The increase in built-up land area in these two vulnerable zones aligns with previous research findings confirming that land use changes in volcanic areas are strongly influenced by population growth dynamics, housing needs, and regional accessibility. Studies in the volcanic region of Semeru and similar areas show that without spatial planning interventions based on disaster risk mitigation, settlements tend to expand toward hazard zones, thereby increasing the risk and vulnerability of the population and infrastructure (Sadono et al., 2017; Bachri et al., 2024). The absence of settlements in Prone Zone III indicates that this area still functions as a natural buffer zone, likely due to extreme geophysical factors or the continued effectiveness of risk buffer zone regulations. The map of built-up land development can be seen in the volcanic eruption hazard zone of Mount Gamalama. The built-up land area within the volcanic eruption hazard zone of Mount Gamalama can be seen in Figure 7 and 8.

The implications of these findings underscore the necessity of integrating spatial-temporal prediction results into spatial planning policies and future disaster risk reduction strategies. Uncontrolled urbanization has been proven to increase exposure and vulnerability to disasters, particularly in areas historically recognized as volcanic red zones. The effectiveness of implementing spatial planning regulations and strengthening risk literacy among communities is key to curbing the expansion of built-up land into highly disaster-prone areas, as proposed in international comparative studies related to urban growth in high-risk zones (Moroz & Thieken, 2024).

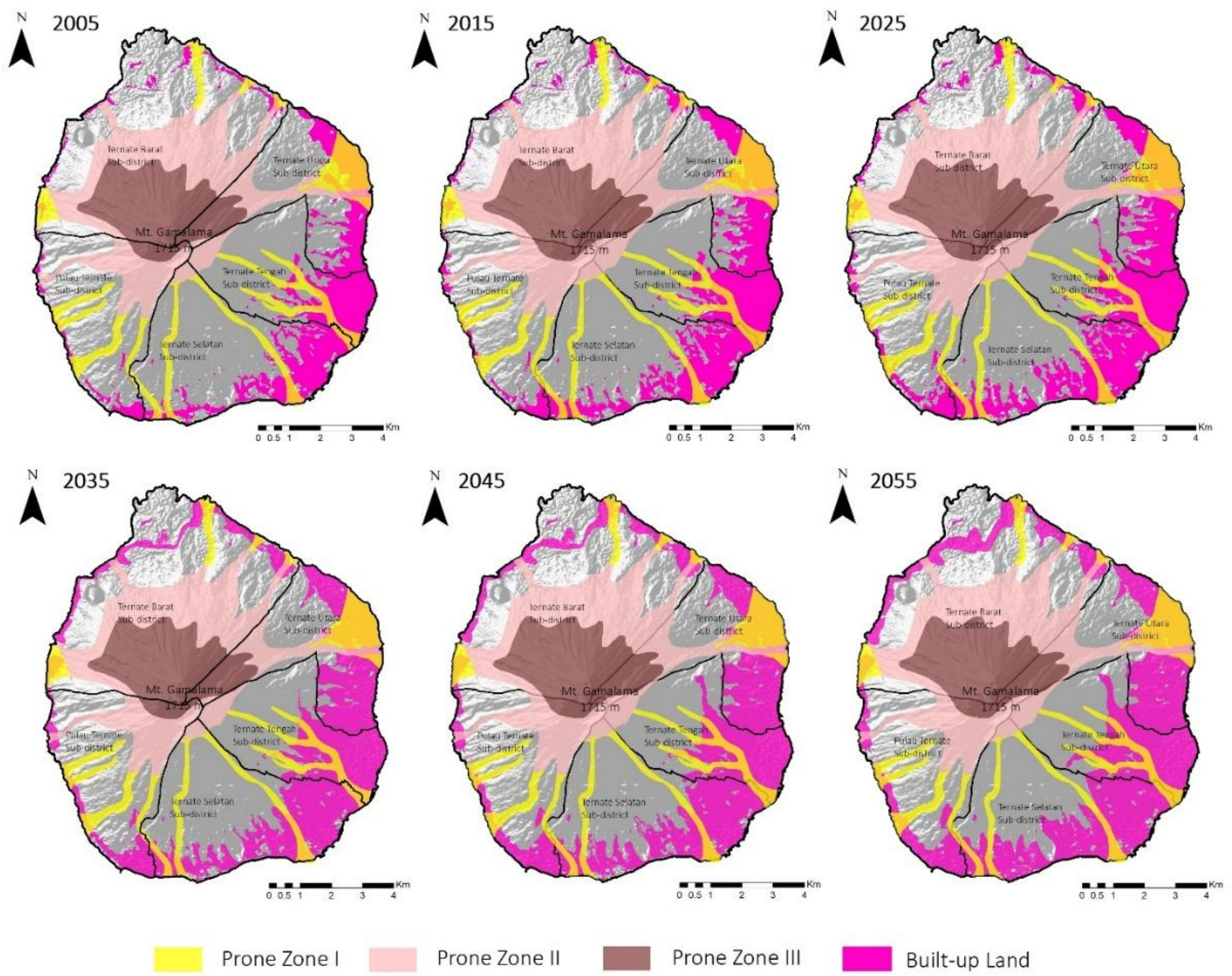

Figure 8. Prediction of Built-up Land Development in the Disaster-Prone Area of Mount Gamalama Volcanic Eruptions

7. Policy Recommendations Related to Disaster Mitigation-Based Spatial Planning in the Volcanic Eruption Hazard Zone of Mount Gamalama

The formulation of policy recommendations must be based on evaluations of previous cases related to disaster management for the Mt. Gamalama eruption, as well as refer to existing regulations and relevant research from experts. This is important to ensure that the resulting policies are responsive, adaptive, and strongly evidence-based. For example, the evaluation of the effectiveness of zoning in the disaster-prone areas I, II, and III implemented in the residential area of Kampung Tubo in Ternate City, as well as the success of evacuation routes and identified shelter facilities, can serve as a foundation for further policy development (Pradiptasari et al., 2015). In addition, policies should also refer to technical guidelines and standards set by relevant agencies such as the Regional Disaster Management Agency (BPBD), Ministry of Energy and Mineral Resources (ESDM), and volcanology institutions, to ensure that spatial planning and risk mitigation align with the actual hazard levels and geographical conditions of Mount Gamalama. This approach guarantees the integration of field experience, national and local regulations, and relevant scientific findings to minimize risks for communities living in eruption hazard zones.

These references support the importance of strengthening risk zoning, enforcing strict regulations on land development in high-risk zones, and ensuring community preparedness through enhanced inter-sectoral coordination and modernization of early warning systems, as has been implemented and analyzed in previous studies and applications on Ternate Island. Thus, the formulation of risk-based mitigation policies is expected to reduce community vulnerability and socio-economic impacts, while achieving safe and sustainable development in the disaster-prone areas of Mount Gamalama.

CONCLUSION

Based on the spatio-temporal analysis of land cover on Ternate Island from 2005 to the projected year 2055, a significant upward trend in built-up land was identified, increasing from 1,543.61 hectares (15.19%) in 2005 to 3,090.05 hectares (30.41%) in 2055, accompanied by a decrease in agricultural land from 8,165.80 hectares (80.35%) to 6,677.53 hectares (65.71%). These changes reflect strong urbanization pressure, particularly in the eruption hazard zones of Mount Gamalama, which increases community vulnerability to volcanic disasters and their socio-economic impacts, including food security risks. Model validation with a kappa index of 0.7643 (76%) indicates a very good accuracy level of the Cellular Automata-Markov Chain method, which effectively captures the dynamics of change and supports long-term predictions. These findings emphasize the need to implement spatial planning policies based on disaster risk mitigation by restricting development in hazard zones, strengthening evacuation infrastructure, and involving local communities in disaster mitigation to ensure sustainable development while reducing exposure to risks on Ternate Island. Future research is recommended to integrate more detailed socio-economic data and additional environmental variables, as well as adopt more advanced modeling techniques such as machine learning to improve prediction accuracy and the effectiveness of risk mitigation in the volcanic hazard areas of Mount Gamalama.

REFERENCES

Abdelsamie , E. A., Mustafa, A. A., El-Sorogy, A. S., Maswada, H. F., Almadani, S. A., Shokr, M. S., El-Desoky, A. I., & Meroño de Larriva, J. E. (2024). Current and potential land use/land cover (lulc) scenarios in dry lands using a ca-markov simulation model and the classification and regression tree (cart) method: A cloud-based google earth engine (GEE) approach. *Sustainability*, *16*(24), 11130. https://doi.org/10.3390/su162411130

Achmadi, P. N., Dimyati, M., Manesa, M. D. M., & Rakuasa, H. (2023). Model perubahan tutupan lahan berbasis CA-Markov: Studi kasus kecamatan Ternate Utara, kota Ternate. *Jurnal Tanah Dan Sumberdaya Lahan*, *10*(2), 451–460. https://doi.org/10.21776/ub.jtsl.2023.010.2.28

Al-Shaar, W., Adjizian Gérard, J., Nehme, N., Lakiss, H., & Buccianti Barakat, L. (2021). Application of modified cellular automata Markov chain model: forecasting land use pattern in Lebanon. *Modeling Earth Systems and Environment*, *7*(2), 1321–1335. https://doi.org/10.1007/s40808-020-00971-y

Bachri, S., Shrestha, R. P., Sumarmi, Irawan, L. Y., Masruroh, H., Prastiwi, M. R. H., Billah, E. N., Putri, N. R. C., Hakiki, A. R. R., & Hidiyah, T. M. (2024). Land use change simulation model using a land change modeler in anticipation of the impact of the Semeru volcano eruption disaster in Indonesia. *Environmental Challenges*, *14*, 100862. https://doi.org/10.1016/j.envc.2024.100862

Badan Standarisasi Nasional. (2010). *SNI 7645-2010 tentang Klasifikasi Penutup Lahan*.

Bastos Moroz, C., & Thieken, A. H. (2024). Urban growth and spatial segregation increase disaster risk: Lessons learned from the 2023 disaster on the North Coast of São Paulo, Brazil. *Natural Hazards and Earth System Sciences*, *24*(9), 3299–3314. https://doi.org/10.5194/nhess-24-3299-2024

BMKG. (2019). *Katalog Tsunami Indonesia Tahun 416-2018 per wilayah*. Badan Meteorologi dan Geofisika.

BPS. (2024). *Kota Ternate Dalam Angka Tahun 2023* (BPS Kota Ternate (ed.)). BPS Kota Ternate.

Cardwell, R., McDonald, G., Wotherspoon, L., & Lindsay, J. (2021). Simulation of post volcanic eruption land use and economic recovery pathways over a period of 20 years in the Auckland region of New Zealand. *Journal of Volcanology and Geothermal Research*, *415*, 107253.

https://doi.org/10.1016/j.jvolgeores.2021.107253

Ervita, K., Marfai, M. A., Khakhim, N., & Mei, E. T. W. (2019). Tsunami susceptibility mapping in the coastal area of Ternate Island. In T. D. Pham, K. D. Kanniah, K. Arai, G. J. P. Perez, Y. Setiawan, L. B. Prasetyo, & Y. Murayama (Eds.), *Sixth International Symposium on LAPAN-IPB Satellite* (p. 107). SPIE. https://doi.org/10.1117/12.2541843

Espitia, H., Soriano, J., Machón, I., & López, H. (2021). Compact fuzzy systems based on boolean relations. *Applied Sciences* (Vol. 11, Issue 4). https://doi.org/10.3390/app11041793

Fachruddin, F., Sanusi, S., Yusra, A., Suhendra, R., Usman, M., & Safriani, M. (2025). Modeling of cellular automata Marcov chain for land use change prediction in Nagan Raya regency. *International Journal of Geoinformatics*, 143–154. https://doi.org/10.4028/p-IZt6M5

Fitri, N. I., Damayanti, A., Indra, T. L. L., & Dimyati, M. (2021). Cellular automata and Markov chain spatial modeling for residential area carrying capacity in Samarinda City, East Kalimantan province. *IOP Conference Series: Earth and Environmental Science*, *673*(1), 12051. https://doi.org/10.1088/1755-1315/673/1/012051

Gandharum, L., Hartono, D. M., Karsidi, A., Ahmad, M., Prihanto, Y., Mulyono, S., Sadmono, H., Sanjaya, H., Sumargana, L., & Alhasanah, F. (2024). Past and future land use change dynamics: assessing the impact of urban development on agricultural land in the Pantura Jabar region, Indonesia. *Environmental Monitoring and Assessment*, *196*(7), 645. https://doi.org/10.1007/s10661-024-12819-4

Gharaibeh, A., Shaamala, A., Obeidat, R., & Al-Kofahi, S. (2020). Improving land-use change modeling by integrating ANN with cellular automata-Markov Chain model. *Heliyon*, *6*(9), e05092. https://doi.org/10.1016/j.heliyon.2020.e05092

Ham, C. M. (2024). Reflecting on the 1775 Mount Gamalama eruption: Lessons from indigenous knowledge for sustainable development in Ternate island, North Maluku province, Indonesia. *Journal of Human Ecology and Sustainability*, *2*(3), 2. https://doi.org/10.56237/jhes24ichspd01

Handayani, W., Mutaqin, B. W., Marfai, M. A., Tyas, D. W., Alwi, M., Rosaji, F. S. C., Hilmansyah, A. A., Musthofa, A., & Fahmi, M. S. I. (2022). Coastal hazard modeling in Indonesia small island: Case study of Ternate island. *IOP Conference Series: Earth and Environmental Science*, *1039*(1), 012025. https://doi.org/10.1088/1755-1315/1039/1/012025

Heinrich Rakuasa. (2025). Classification of Sentinel-2A satellite image for Ternate city land cover using random forest classification in SAGA GIS Software. *DNS – Digital Nexus Systematic Journal*, *1*(1), 34–36. http://dx.doi.org/10.26753/dns.v1i1.1554

Hidayat, A., Marfai, M. A., & Hadmoko, D. S. (2022). The 2015 eruption of Gamalama volcano (Ternate Island–Indonesia): precursor, crisis management, and community response. *GeoJournal*, *87*(1), 1–20. https://doi.org/10.1007/s10708-020-10237-w

Jafarpour Ghalehteimouri, K., Shamsoddini, A., Mousavi, M. N., Binti Che Ros, F., & Khedmatzadeh, A. (2022). Predicting spatial and decadal of land use and land cover change using integrated cellular automata Markov chain model based scenarios (2019–2049) Zarriné-Rūd River Basin in Iran. *Environmental Challenges*, *6*, 100399. https://doi.org/10.1016/j.envc.2021.100399

Kamarajugedda, S. A., Johnson, J. A., McDonald, R., & Hamel, P. (2023). Carbon storage and sequestration in Southeast Asian urban clusters under future land cover change scenarios (2015–2050). *Frontiers in Environmental Science*, *11*. https://doi.org/10.3389/fenvs.2023.1105759

Kura, A. L., & Beyene, D. L. (2020). Cellular automata Markov chain model based deforestation modelling in the pastoral and agro-pastoral areas of southern Ethiopia. *Remote Sensing Applications: Society and Environment*, *18*, 100321. https://doi.org/10.1016/j.rsase.2020.100321

Kusrini, Worosuprojo, S., Kurniawan, A., & Hizbaron, D. R. (2023). Land use changes of Ternate island 2017-2022. *E3S Web of Conferences*, *468*, 10005. https://doi.org/10.1051/e3sconf/202346810005

Latue, P. C., & Rakuasa, H. (2024). Land cover change analysis of Ternate Selatan sub-district, Ternate city in 2014 and 2024. *International Journal of Selvicoltura Asean*, *1*(1), 17–22. https://journal.ypidathu.or.id/index.php/selvicoltura/article/view/861

Lessy, M. R., Lassa, J., & Zander, K. K. (2024). Understanding multi-hazard interactions and impacts on small-island communities: Insights from the Active Volcano Island of Ternate, Indonesia. *Sustainability*, *16*(16), 6894. https://doi.org/10.3390/su16166894

Ma'muri, Santoso, I., Sudiro, A., & Maryanto, S. (2025). Assessing vulnerability in the face of multiple hazards: Insights from a literature review on Indonesia's disaster risk management. *IOP Conference Series: Earth and Environmental Science*, *1486*(1), 12041. https://doi.org/10.1088/1755-1315/1486/1/012041

Mao, F., Li, X., Zhou, G., Huang, Z., Xu, Y., Chen, Q., Yan, M., Sun, J., Xu, C., & Du, H. (2023). Land use and cover in subtropical East Asia and Southeast Asia from 1700 to 2018. *Global and Planetary Change*, *226*, 104157. https://doi.org/10.1016/j.gloplacha.2023.104157

Marasabessy, F. (2016). Hirarki wilayah kota Ternate Pasca pengembangan kawasan waterfront city. *Jurnal Wilayah Dan Lingkungan*, *4*(3), 213. https://doi.org/10.14710/jwl.4.3.213-224

Mirzakhani, A., Behzadfar, M., & Azizi Habashi, S. (2025). Simulating urban expansion dynamics in Tehran through satellite imagery and cellular automata Markov chain modelling. *Modeling Earth Systems and Environment*, *11*(2), 145. https://doi.org/10.1007/s40808-025-02325-y

Philia Christi Latue, & Heinrich Rakuasa. (2023). Spatial dynamics of land cover change in Wae Batu Gantung watershed, Ambon city, Indonesia. *International Journal of Scientific Multidisciplinary Research*, *1*(3), 117–130. https://doi.org/10.55927/ijsmr.v1i3.3623

Pradiptasari, A. G., Waani, J. O., & Mononimbar, W. (2015). Sistem penanggulangan bencana gunung api Gamalama di permukiman kampung Tubo Kota Ternate. *Spasial*, *2*(3), 33–42. https://doi.org/10.35793/sp.v2i3.9828

Rakuasa, H., & Pakniany, Y. (2022). Spatial dynamics of land cover change in Ternate Tengah district, Ternate city, Indonesia. *Forum Geografi*, *36*(2), 126–135. https://doi.org/DOI: 10.23917/forgeo.v36i2.19978

Rakuasa, H. (2025). Spatial analysis of built-up land development in 2019 and 2024 based on slope level in Ternate City Indonesia. *Proceeding of Geo Tourism International Conference*, 1–8.

Rakuasa, H., & Khromykh, V. V. (2025). Simulation of urban growth in Ternate island using cellular automata Markov chains models. *Asian Journal of Environmental Research*, *2*(1), 101–114. https://doi.org/10.69930/ajer.v2i1.310

Sadono, R., Hartono, H., Machfoedz, M. M., & Setiaji, S. (2017). Monitoring land cover changes in the disaster-prone area: A case study of Cangkringan sub-district, the flanks of mount Merapi, Indonesia. *Forum Geografi*, *31*(2), 209–219. https://doi.org/10.23917/forgeo.v31i2.5324

Salakory, M., Rakuasa, H. (2022). Modeling of cellular automata Markov chain for predicting the carrying capacity of Ambon city. *Jurnal Pengelolaan Sumberdaya Alam Dan Lingkungan (JPSL)*, *12*(2), 372–387. https://doi.org/https://doi.org/10.29244/jpsl.12.2.372-387

Sihasale, D. A., Latue, P. C., & Rakuasa, H. (2023). Spatial analysis of built-up land suitability in Ternate Island. *Jurnal Riset Multidisiplin Dan Inovasi Teknologi*, *1*(02), 70–83. https://doi.org/10.59653/jimat.v1i02.219

Somae, G., Supriatna, S., Rakuasa, H., & Lubis, A. R. (2023). Pemodelan spasial perubahan tutupan lahan dan prediksi tutupan lahan kecamatan Teluk Ambon Baguala menggunakan CA-Markov. *Jurnal Sains Informasi Geografi (J SIG)*, *6*(1), 10–19. http://dx.doi.org/10.31314/jsig.v6i1.1832

Supriatna, S., Mukhtar, M. K., Wardani, K. K., Hashilah, F., & Manessa, M. D. M. (2022). CA-Markov chain model-based predictions of land cover: A case study of Banjarmasin city. *Indonesian Journal of Geography*, *54*(3). https://doi.org/10.22146/ijg.71721

Tyas Wulan Mei, E., Meilyana Sari, I., Fajarwati, A., & Safitri, D. (2017). Assessing the social economic and physical vulnerabilities to Gamalama volcano. *Proceedings of the Lst*

International Cohference on Geography and Education (ICGE 2016). https://doi.org/10.2991/icge-16.2017.7

Ubink, J., & Pickering, J. (2024). The mine, the community, and the chief–mining governance and community representation in conditions of legal pluralism. *Legal Pluralism and Critical Social Analysis*, 1–29. https://doi.org/10.1080/27706869.2024.2372898

Umanailo, H. A., Franklin, P. J., & Waani, J. O. (2017). Perkembangan pusat kota Ternate (Studi Kasus: Kecamatan Ternate Tengah). *Spasial*, *4*(3), 222–233.

Wang, Q., Wang, H., Chang, R., Zeng, H., & Bai, X. (2022). Dynamic simulation patterns and spatiotemporal analysis of land-use/land-cover changes in the Wuhan metropolitan area, China. *Ecological Modelling*, *464*, 109850. https://doi.org/10.1016/j.ecolmodel.2021.109850

Xing, W., Qian, Y., Guan, X., Yang, T., & Wu, H. (2020). A novel cellular automata model integrated with deep learning for dynamic spatio-temporal land use change simulation. *Computers & Geosciences*, *137*, 104430. https://doi.org/10.1016/j.cageo.2020.104430

Yaagoubi, R., Lakber, C.-E., & Miky, Y. (2024). A comparative analysis on the use of a cellular automata Markov chain versus a convolutional LSTM model in forecasting urban growth using sentinel 2A images. *Journal of Land Use Science*, *19*(1), 258–277. https://doi.org/10.1080/1747423X.2024.2403789

Yuliantina, N., Mulyana, A., Wildayana, E., & Lionardo, A. (2024). Economic impact of land use change on rice paddy farmers in Palembang city Indonesia. *Wseas Transactions on Environment and Development*, *20*, 546–561. https://doi.org/10.37394/232015.2024.20.53